Short communication

Desirable performance of intermediate-temperature solid oxide fuel cell with an anode-supported $La_{0.9}Sr_{0.1}Ga_{0.8}Mg_{0.2}O_{3-\delta}$ electrolyte membrane

Wenbao Wang [a,b], Zhijie Yang [a], Hongtao Wang [a], Guilin Ma [a,*], Weijian Gao [b], Zhufa Zhou [a,*]

[a] Key Laboratory of Organic Synthesis of Jiangsu Province, College of Chemistry, Chemical Engineering and Materials Science, Soochow University, Suzhou 215123, China
[b] Center of Analysis and Testing, Soochow University, Suzhou 215123, China

ARTICLE INFO

ABSTRACT

An anode-supported $La_{0.9}Sr_{0.1}Ga_{0.8}Mg_{0.2}O_{3-\delta}$ (LSGM) electrolyte membrane is successfully fabricated by simple, cost-effective spin coating process. Nano-sized NiO and $Ce_{0.8}Gd_{0.2}O_{3-\alpha}$ (GDC) powders derived from precipitation and citric-nitrate process, respectively, are used for anode support. The dense and uniform LSGM membrane of ca. 50 μm in thickness is obtained by sintering at relatively low temperature 1300 °C for 5 h. A single cell based on the as-prepared LSGM electrolyte membrane exhibits desirable high cell performance and generates high output power densities of 760 mW cm^{-2} at 700 °C and 257 mW cm^{-2} at 600 °C, respectively, when operated with humidified hydrogen as the fuel and air as the oxidant. The single cell is characterized by field-emission scanning electron microscope (FESEM), X-ray diffraction (XRD) and electrochemical AC impedance. The results demonstrate that it is feasible to fabricate dense LSGM membrane for solid oxide fuel cell by this simple, cost-effective and efficient process. In addition, optimized anode microstructure significantly reduces polarization resistance (0.025 Ω cm^2 at 700 °C).

© 2010 Elsevier B.V. All rights reserved.

1. Introduction

The chemical energy in fuels can be directly converted into electricity by electrochemical devices – solid oxide fuel cells (SOFCs) [1,2]. Y_2O_3 stabilized ZrO_2 (YSZ) electrolyte is often applied in SOFCs due to its good chemical stability, high-mechanical stability and pure ionic conduction. However, relatively high operating temperature (between 800 °C and 1000 °C) can lead to not only high fabrication cost for SOFCs systems, but also complex material problems including electrode sintering, interfacial diffusion between electrolyte and electrodes, and mechanical stress due to the different thermal expansion coefficients. Therefore, from a practical application point of view, intermediate-temperature solid oxide fuel cells (IT-SOFCs) (below 800 °C) have been an inevitable trend of commercializing development for wide material selection, long life, and low manufacturing cost [2–5]. On the other hand, a decrease in the operating temperature will result in a loss of output power density due to significant reduction of both ionic conduction of the electrolyte and catalytic activity of the electrodes. Therefore, decreasing the thickness of the electrolyte and optimizing elec-trode microstructure have been two optional ways to reduce cell resistance loss and improve cell performance.

A number of techniques have been developed to prepare thin electrolyte membranes, such as electrophoretic deposition [5,6], screen-printed deposition [7], pulse laser deposition [8,9], dry-pressing method [10,11], electrostatic spray deposition [12], RF sputtering [13] and spin coating method [14] etc. In spite of high deposition rate, it is difficult to obtain a dense thin electrolyte membrane by electrostatic spray deposition. Some deposition methods such as pulse laser deposition and RF sputtering are complex, time-consuming, expensive and difficult to deposit relatively thick, uniform and dense films. Spin-coating process is a simple, cost-effective and efficient method and suitable for mass-production, and recently has been developed successfully to fabricated the various solid electrolyte membranes for fuel cells and electrochemical reactors [14–16]. The thickness of the thin electrolyte membrane can be easily controlled by viscosity of slurry, spin-coating velocity and repeating times.

In a hydrogen/oxygen solid oxide fuel cell based on a mixed ion (oxide-ion + proton) conductor, instead of the oxygen ionic or pro-tonic conduction, the total ionic conduction determines fuel cell performance. Thus it is important to choose a suitable electrolyte material with good ionic conduction. Perovskite-type LSGM materials are often regarded as a promising family of electrolyte for IT-SOFCs due to their superior oxygen ionic and protonic conductivities, good chemical stability and especially, high ionic transference

* Corresponding author at: College of Chemistry, Chemical Engineering and Materials Science, Dushu Lake Campus of Soochow University, Suzhou 215123, China. Tel.: +86 512 65880326; fax: +86 512 65880089.
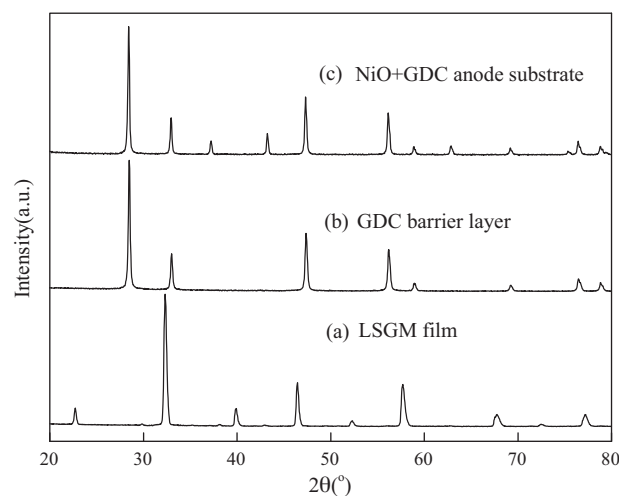E-mail address: 32uumagl@suda.edu.cn (G. Ma).

number in the intermediate temperature range [17–19]. Recently, considerable research work has been devoted to developing thin LSGM membrane fuel cell with high output power density capable of operating in the intermediate temperature range. Bi et al. fabricated an anode-supported SOFC with LDC ($\sim$25 μm) and LSGM ($\sim$75 μm) bi-layer electrolytes by dry-pressing process. The maximum power densities of 1100 mW cm^{-2} and 560 mW cm^{-2} at 800 °C and 700 °C, respectively, were obtained. LDC was introduced to minimize reactions between LSGM and the anode support [11]. Ju et al. fabricated a SOFC based on LSGM film deposited by pulsed laser deposition on Ni–Fe bimetallic porous anode support. The cell showed high cell performance and the maximum power densities were 1790, 820 and 290 mW cm^{-2} at 700, 600 and 500 °C, respectively [9]. Bozza et al. reported an anode-supported IT-SOFC with a LSGM film deposited by electrophoretic deposition with remarkable power densities (780 mW cm^{-2} at 700 °C and 275 mW cm^{-2} at 600 °C) [5]. However, to date there is little information available on LSGM membrane prepared via spin-coating process. In the present work, we report the fabrication of anode-supported LSGM membranes via spin coating process. Nano-sized NiO and Ce$_{0.8}$Gd$_{0.2}$O$_{3-\alpha}$ (GDC) powders derived from precipitation and citric-nitrate process, respectively, were used for anode supports. After sintering at relatively low temperature 1300 °C for 5 h, uniform and extremely dense anode-supported LSGM membranes (ca. 50 μm) were obtained. The desirable output power densities, which were observed on a single cell with an as-prepared LSGM membrane at intermediate temperatures, demonstrated high-quality LSGM membrane on Ni–GDC anode support with a GDC barrier layer.

2. Experimental

LSGM precursor powders were prepared by citric-nitrate process. All the reagents used are analytical-grade (A.R.). The stoichiometric quantities of La(NO$_3$)$_3$·6H$_2$O, Sr(NO$_3$)$_2$, Ga(NO$_3$)$_3$ (metal Ga was dissolved into dilute HNO$_3$) and Mg(NO$_3$)$_2$·6H$_2$O were dissolved in deionized water under stirring and citric acid was added as the complexant with a mol ratio of citric acid: metal = 1.5. Then the solution was heated under stirring, evaporated to form a viscous gel and ignited to flame. The LSGM powders were obtained by calcining the resultant ash at 1100 °C for 8 h. The similar process was applied to prepare GDC powders. Required amounts of Gd(NO$_3$)$_3$·6H$_2$O, Ce(NH$_4$)$_2$(NO$_3$)$_6$ were mixed in deionized water, and then citric acid was added at a citric acid to metal molar ratio of 2:1 to prepare an GDC solution. Then the solution was heated on a hot plate to vaporize water, converted into gel and ignited to flame. Subsequently, the yellow ash was fired at 600 °C for 2 h to obtain GDC powders. NiO powders were synthesized by precipitation process. Ni(NO$_3$)$_2$·6H$_2$O (A.R.) was dissolved in deionized water and ammonia (A.R.) solution was added drop by drop under stirring at room temperature. The molar ratio of Ni^{2+} to NH$_3$·H$_2$O was 1:2. The mixture was aged at 70 °C for 4 h and filtrated. The resultant precipitate was subsequently dried at 100 °C, followed by calcining at 400 °C for 2 h to get nickel oxide powders. As-prepared NiO and GDC powders were confirmed by TEM to be nano-sized. The nano-sized GDC and NiO powders were blended with a weight ratio of 35:65 using ball-milling in ethanol for 2 h. To form sufficient porosity in anode supports, 10 wt.% starch was added as pore former. The well-mixed powders were pressed into green pellets of 13 mm in diameter and 0.8 mm in thickness under 50 MPa, followed by firing at 1000 °C for 4 h as anode supports. Ba$_{0.5}$Sr$_{0.5}$Co$_{0.8}$Fe$_{0.2}$O$_{3-\beta}$ (BSCF), prepared as described in [16], was used as cathode material.

The as-prepared LSGM and GDC powders passed through a sieve (500 mesh) to get uniform powders. Homogeneous and stable LSGM slurry was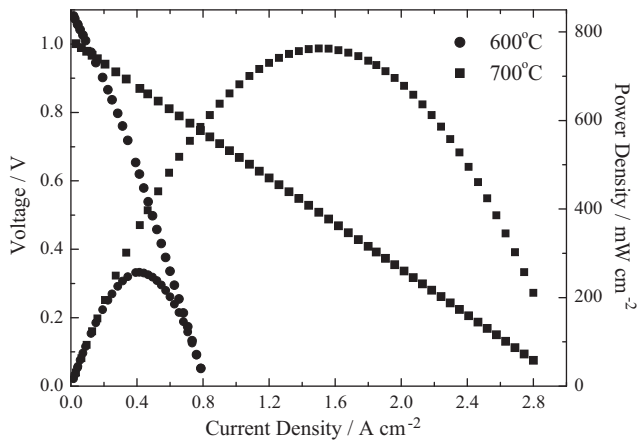 prepared by mixing LSGM powders with a homemade organic binder consisting of ethyl cellulose (A.R.) and terpineol (A.R.), respectively. The weight ratio of powder to the organic binder was 1. The GDC slurry was prepared by a similar process.

Then, spin coating process was applied to prepare GDC barrier layer and electrolyte layer. The GDC slurry was first spin-coated onto the pre-sintered NiO–GDC anode supports. After dried for 30 min, LSGM electrolyte layers were deposited on the GDC barrier layers by spin coating at 3500 rpm for 60 s followed by heat treatment. The spin coating process was repeated three times in order to ensure that dense and uniform electrolyte membrane with adequate thickness was obtained for electrochemical measurement. After sintering at 1300 °C for 5 h at a heating rate of 2 °C min^{-1}, trilayer half cells were obtained. The BSCF paste was coated onto the pre-sintered membrane and sintered at 1000 °C for 2 h. The surface area was ca.0.5 cm^2. Ag–Pd paste was painted on two surfaces (ca. 0.5 cm^2), dried by an infrared lamp and then fired at 800 °C for 20 min as current collectors.

At the anode side of the single cell, a molten Pyrex glass in the homemade furnace was used as the ceramic binding agent to seal the single cell to an alumina tube. The cathode was exposed to ambient air. The current–voltage curve was measured to evaluate the cell performance in the intermediate temperature range (600–700 °C). Humidified hydrogen was used as the fuel, and ambient air as the oxidant. The volumetric flow rate of the humidified hydrogen was 100 ml min^{-1}. The cell performance and electrochemical impedance spectra were determined by an electrochemical workstation (Zahner IM6ex). The impedance spectra were collected under open circuit conditions over a frequency range of 1 Hz to 3 MHz. The microstructure of the single cell after electrochemical testing was observed by a FESEM (Hitachi S-4700). The phases of all samples were identified by XRD on a Panalytical X'pert Pro MPD diffractometer with an X' Celerator detector.

3. Results and discussion

The phase compositions of LSGM membrane system were determined by XRD. The XRD pattern shown in Fig. 1a indicates that the LSGM membrane sintered at 1300 °C for 5 h was well-crystallized as a perovskite-type LSGM phase. As shown in Fig. 1b, the GDC barrier layer after calcining at 1000 °C presented a single phase without formation of an impurity phase. Fig. 1c presents the XRD pattern of anode support GDC–NiO (weight ratio of 35:65) sintered at 1300 °C

Fig. 1. XRD patterns for (a) LSGM electrolyte membrane sintered at 1300 °C for 5 h, (b) the GDC barrier layer calcined at 1000 °C for 5 h, and (c) NiO–GDC anode support, respectively.

Fig. 2. *I–V* curves of the membrane fuel cell operated on humidified hydrogen (anode) and ambient air (cathode) atmospheres at intermediate temperatures.

for 5 h. It can be clearly seen that there were only peaks corresponding well to a mixture of GDC and NiO. It indicates that GDC and NiO did not react with each other during the sintering process.

A single cell was assembled with an as-prepared LSGM electrolyte membrane. Fig. 2 shows the current–voltage characteristics and the corresponding power densities of the LSGM membrane (~50 μm) fuel cell. The open circuit voltages (OCVs) of the membrane fuel cell were 1.00 V at 700 °C, and 1.02 V at 600 °C, respectively. The measured OCVs at different given temperatures are higher than the values of the cell based on LSGM electrolyte reported by He et al. [20], an indication of sufficiently dense electrolyte membrane.

The maximum output power densities of the membrane fuel cell were 760 mW cm^{-2} at 700 °C and 257 mW cm^{-2} at 600 °C, respectively, which are higher than the anode-supported fuel cells with a LSGM membrane of ca. 15 μm reported in the literature [20] and close to the values (with the thickness of ca. 30 μm) reported [5]. The performance is also better than that of the cell with LSGM electrolyte (75 μm) prepared by classical dry-pressing method at corresponding temperatures [10]. An anode-supported SOFC with a ca. 30 μm-thick LDC/LSGM/LDC tri-layer deposited on a NiO–LDC anode substrate by colloidal deposition method was fabricated by Lin and Barnett [21]. The maximum power densities measured for their cell were 910 mW cm^{-2} and 600 mW cm^{-2} at 700 °C and 600 °C, respectively, slightly higher than our results. The differences may be attributed to different resistance losses due to different electrolyte membrane and electrode microstructures. The desirable results also demonstrate that it is feasible to prepare thin and dense LSGM electrolyte membrane by the simple and cost-effective spin coating process.

Fig. 3a–c shows the cross-sectional FESEM images of the LSGM membrane fuel cell system after electrochemical testing. Fig. 3a shows that the thickness of the membrane was uniform and around 50 μm and the LSGM membrane adhered to the barrier layer and the cathode firmly. The electrolyte membrane, as shown in the high-resolution image Fig. 3b, was sufficiently dense. Combined with XRD results, it is interesting to note that the electrolyte could be densified after sintering at relatively low temperature 1300 °C, which may be ascribed to the favorable effects of the membrane surface tension and the fluidity of slurry. To overcome the variation in thickness of LSGM electrolyte layer due to non-uniform particle distribution in the slurry, LSGM powders after ball milling passed though a 500 mesh sieve. Fig. 3c presents the microstructure of the cross-section of the Ni–GDC anode support after testing. The micrograph indicates that Ni (white gray) in the anode support after reducing was extremely porous, which is quite suitable for
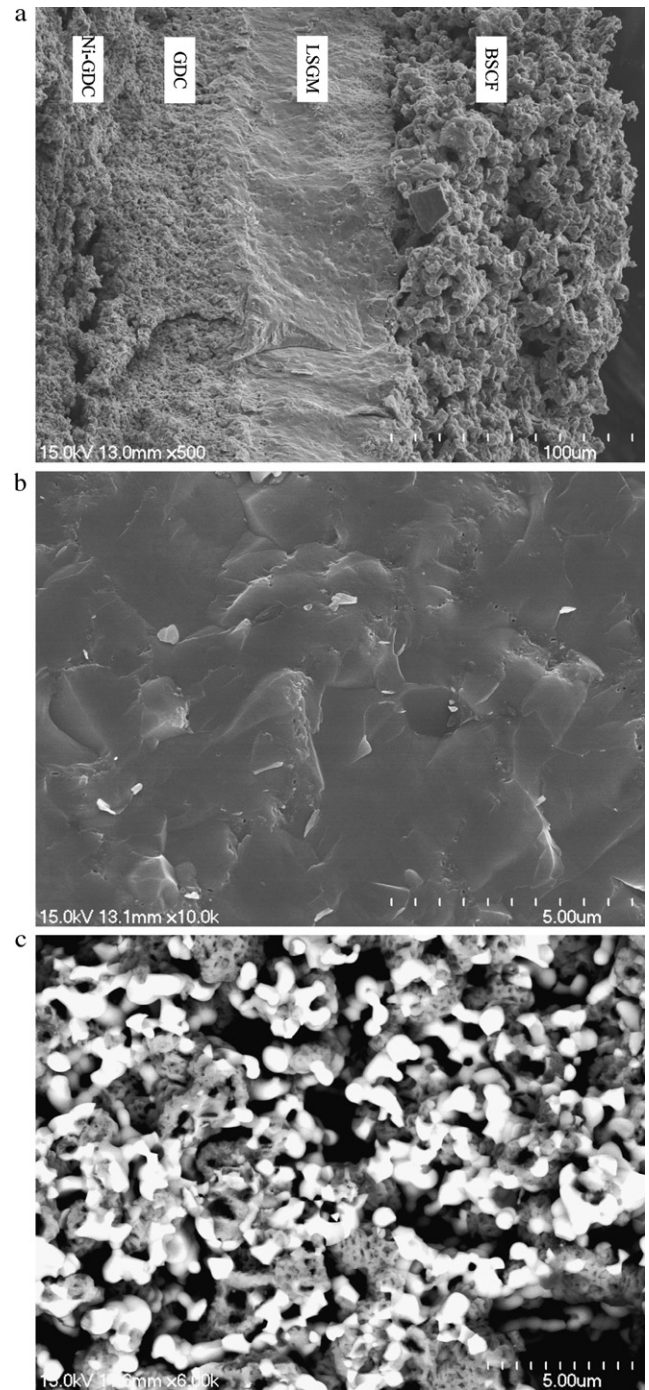
Fig. 3. (a) SEM micrograph of the cross sectional view of the as-prepared membrane fuel cell, Ni–GDC/GDC/LSGM/BSCF, after testing. (b) High-resolution microscopic view of cross section of LSGM membrane. (c) Cross-section view of Ni–GDC anode support after testing.

gas phase diffusion. Porous Ni will exhibit better chemisorption properties and serve as a better electrocatalyst for electrochemical reaction of hydrogen. Therefore it will effectively broaden the three-phase boundaries. Additionally, as also shown in Fig. 3c, a highly porous Ni/GDC cermet anode will enlarge a surface area to aid its effectiveness. In the hydrogen/air fuel cell, LSGM ceramics can conduct proton and oxygen ions [17–19], and the proton and oxygen ion conduction dominates the whole fuel cell performance. Therefore, the porous framework can aid gas diffusion, thus effectively reducing polarization resistance and improving the cell
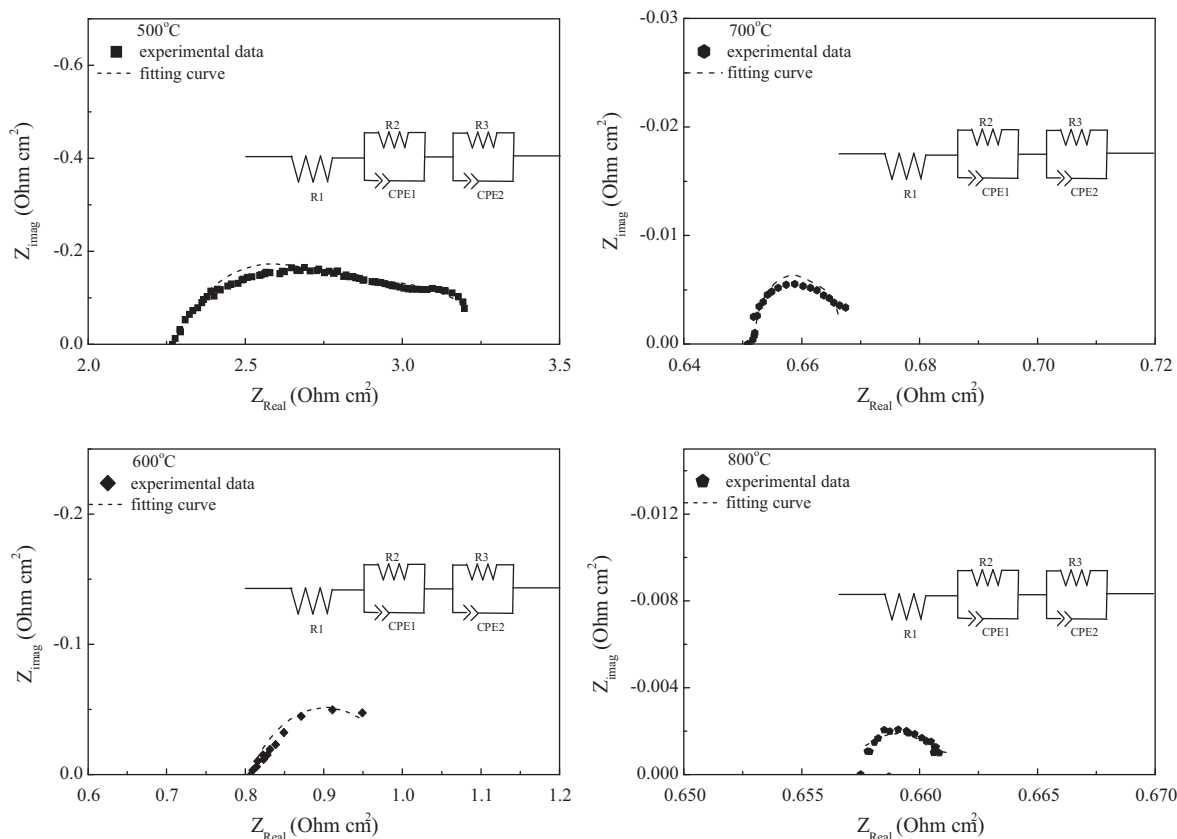
Fig. 4. The impedance spectra of LSGM membrane fuel cell at different temperatures. Impedance was measured under open-circuit conditions in humidified hydrogen (anode) with a flow rate of 100 ml min^{-1} and ambient air (cathode). The dash lines are fitting curves of equivalent circuits of the inset.

performance. On the other hand, as we all know, GDC is an excellent mixed conductor in reducing atmosphere. Therefore, an introduction of porous barrier layer GDC will result in a substantial increase in the ionic conductivity of fuel cell system and further increase hydrogen oxidation rate.

The impedance spectra of the membrane fuel cell under open circuit conditions at different temperatures are shown in Fig. 4. The impedance spectra were modeled with the equivalent circuit of the inset by software ZView 3.0a. The total area specific resistance R_t, the area specific electrolyte resistance R_s and the area specific polarization resistance R_p derived from the fitting results are shown in Fig. 5. R_t could be determined from the intercept on the real axis
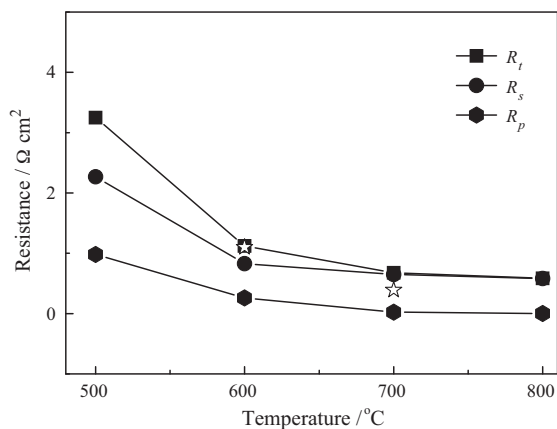
Fig. 5. The total area specific resistance R_t, area specific electrolyte resistance R_s, and area specific polarization resistance R_p determined from the impedance spectra. The slopes of V–I curves are symbolized with ☆.

at low frequencies. The higher frequency intercept on the real axis represents R_s. The difference between R_t and R_s corresponds to the polarization resistance R_p. An increase of temperature resulted in a remarkable decline of R_p and R_s, typically R_p from 0.98 Ω cm^2 at 500 °C to 0.025 Ω cm^2 at 700 °C and R_s from 2.27 Ω cm^2 at 500 °C to 0.67 Ω cm^2 at 700 °C, respectively. It could be observed that in the intermediate temperature range R_s were always higher than R_p. The result indicates that under the present conditions R_s is a dominant factor to determine the performance of the anode-supported LSGM membrane fuel cell. Obviously, the result also coincides with that of SEM analysis. The lower electrode polarization resistance would be attributed to the desirable electrode microstructure [22]. Therefore, the performance of LSGM membrane fuel cells can be further improved by the reduction of electrolyte thickness. In addition, as also shown in Fig. 5, the slopes of I–V curves were close to R_t at corresponding temperatures. The small differences between the two may be ascribed to the interdiffusion of cations and undesired reactions after long-time electrochemical testing, which will result in performance degradation of the membrane fuel cell [23].

4. Conclusions

A simple and cost-effective spin coating process was applied to deposit LSGM membrane on porous NiO–GDC anode support with a GDC barrier layer. After co-sintering at relatively low temperature 1300 °C for 5 h, a dense and uniform electrolyte membrane with the thickness of ca. 50 μm was obtained. An anode-supported LSGM membrane fuel cell with BSCF cathode was assembled and tested from 600 °C to 700 °C using humidified hydrogen as the fuel and ambient air as the oxidant. The OCV values reached 1.00 V at 700 °C, and 1.02 V at 600 °C, respectively. The maximum power densities were 760 mW cm^{-2} at 700 °C and 257 mW cm^{-2} at 600 °C,

respectively. In addition, the AC impedance analysis of the single cell demonstrated desirable low electrode polarizations. In conclusion, the spin coating process has been confirmed to be an effective method to prepare thin LSGM electrolyte membrane for IT-SOFCs.

Acknowledgement

References

[1] O. Yamamoto, Electrochim. Acta 45 (2000) 2423–2435.
[2] B.C.H. Steele, Solid State Ionics 75 (1995) 157–165.
[3] T. Ishihara, M. Honda, T. Shibayama, H. Minami, Y. Takita, J. Electrochem. Soc. 145 (1998) 3177–3183.
[4] C.R. Xia, M.L. Liu, Solid State Ionics 144 (2001) 249–255.
[5] F. Bozza, R. Polini, E. Traversa, Electrochem. Commun. 11 (2009) 1680–1683.
[6] I.N. Sora, R. Pelosato, A. Simone, L. Montanaro, F. Maglia, G. Chiodelli, Solid State Ionics 177 (2006) 1985–1989.
[7] J.W. Yan, Z.G. Lu, Y. Jiang, Y.L. Dong, C.Y. Yu, W.Z. Li, J. Electrochem. Soc. 149 (2002) A1132–A1135.
[8] S. Kanazawa, T. Ito, K. Yamada, T. Ohkubo, Y. Nomoto, T. Ishihara, Y. Takita, Surf. Coat. Technol. 169–170 (2003) 508–511.
[9] Y.W. Ju, H. Eto, T. Inagaki, S. Ida, T. Ishihara, J. Power Sources 195 (2010) 6294–6300.
[10] L. Yang, C.D. Zuo, M.L. Liu, J. Power Sources 195 (2010) 1845–1848.
[11] Z. Bi, B.L. Yi, Z.W. Wang, Y.L. Dong, H.J. Wu, Y.C. She, M.J. Cheng, Electrochem. Solid State Lett. 7 (2004) A105–A107.
[12] I. Taniguchi, R.C. van Landschoot, J. Schoonman, Solid State Ionics 160 (2003) 271–279.
[13] K. Sasaki, M. Muranaka, A. Suzuki, T. Terai, Solid State Ionics 179 (2008) 1268–1272.
[14] R. Hui, Z.W. Wang, S. Yick, R. Maric, D. Ghosh, J. Power Sources 172 (2007) 840–844.
[15] N. Ai, Z. Lu, K.F. Chen, X.Q. Huang, Y.W. Liu, R.F. Wang, W.H. Su, J. Membr. Sci. 286 (2006) 255–259.
[16] W.B. Wang, X.B. Cao, W.J. Gao, F. Zhang, H.T. Wang, G.L. Ma, J. Membr. Sci. 360 (2010) 397–403.
[17] T. Ishihara, H. Matsuda, Y. Takita, J. Am. Chem. Soc. 116 (1994) 3801–3803.
[18] K.Q. Huang, S.R. Tichy, J.B. Goodenough, J. Am. Ceram. Soc. 81 (1998) 2581–2585.
[19] G.L. Ma, F. Zhang, J.L. Zhu, G.Y. Meng, Chem. Mater. 18 (2006) 6006–6011.
[20] T.M. He, Q. He, L. Pei, Y. Ji, J. Liu, J. Am. Ceram. Soc. 89 (2006) 2664–2667.
[21] Y.B. Lin, S.A. Barnett, Electrochem. Solid State Lett. 9 (2006) A285–A288.
[22] W.Z. Zhu, S.C. Deevi, Mater. Sci. Eng. A 362 (2003) 228–239.
[23] P.N. Huang, A. Horkey, A. Petric, J. Am. Ceram. Soc. 82 (1999) 2402–2406.